IOP Conference Series: Materials Science and Engineering

First-principles study on electronic structure and photoelectric properties of zinc blende $In_x Ga_{1-x} N$ with different in doping concentrations

IOP Conf. Series: Materials Science and Engineering **504** (2019) 012080 doi:10.1088/1757-899X/504/1/012080

First-principles study on electronic structure and photoelectric properties of zinc blende $In_xGa_{1-x}N$ with different in doping concentrations

Z M Tang, J H Liu, Y L Liu, H He*, Y C Fu and X M Shen

Guangxi Key Laboratory of Processing for Non-ferrous Metallic and Featured Materials, School of Resources, Environment and Materials, Guangxi University, Nanning, 530004, China

Corresponding author and e-mail: H He, noblehe@gxu.edu.cn

Abstract. The first-principles ultra-soft pseudopotential plane wave based on density functional theory is used to calculate the electronic structure and photoelectric properties of zinc blende GaN and zinc blende $In_xGa_{1-x}N$ with different In doping concentrations (x=0, 0.125, 0.25, 0.375, 0.5). It is shown that zinc blende GaN and its In-doped system are all direct bandgap semiconductor materials. With the increase of In doping concentration, the lattice constant of $In_xGa_{1-x}N$ increases and the band gap decreases, the absorption spectrum shift to the red region. Therefore, it can be inferred that by adjusting the doping concentration of In, the light absorption range of $In_xGa_{1-x}N$ can cover the entire solar spectrum, which means that $In_xGa_{1-x}N$ can be worthy to fabricate photovoltaic devices such as full-spectrum solar cells.

1. Introduction

Gallium nitride (GaN) has attract lots of attention for optoelectronic applications due to its excellent properties. Meanwhile, In doping in GaN can further improve the photoelectron properties and the band gap of hexagonal wurtzite $In_xGa_{1-x}N$ alloys can be continuously adjusted from 0.7eV (InN) to 3.4eV (GaN) [1], which means that the $In_xGa_{1-x}N$ alloys can absorb photons at various frequencies in the solar spectrum, providing a material basis for efficient photoelectric conversion.

It is well known that wurtzite structure is more stable than zinc blende structure at room temperature. For this reason, high quality wurtzite structure GaN (wz-GaN) films have been well prepared already [2-4], while zinc blende structure GaN (zb-GaN) films were relatively less studied. Since cubic crystals have higher crystallographic symmetry than hexagonal crystals, the zb-GaN will exhibit a lower phonon scattering [5] and also avoid polarization effects in application. Studies have shown that high In content to GaN is very difficult but necessary in solar cell applications [6], suggesting that zinc blende structure can allow lower doping to get the required properties. However, the growth of pure cubic nitride is difficult due to the metastable nature of the cubic phase in experimental. For the limitation, in this work, the electronic structure and photoelectric properties of zb-GaN and In-doped zinc blende $In_xGa_{1-x}N$ at normal temperature and zero pressure are mainly discussed, and theoretical preparations are made for the further study of epitaxial growth of thin zb-GaN films.

2. Calculation model and method

2.1. Calculation model

The zb-GaN crystal belongs to the F-43m space group, which structure can be understood as two sets of face-centered cubic lattices translated diagonally by 1/4. The lattice parameter of the crystal is a=b=c=4.46 Å, α=β=γ=90°. As shown in Figure 1, a 1×1×2 supercell model is constructed. In order to study the electronic structure and photoelectric properties of zinc blende $In_xGa_{1-x}N$ with different In doping concentrations, a series of doping ratios (x=0, 0.125, 0.25, 0.375, 0.5) are discussed.

2.2. Calculation method

The calculations are based on Density functional theory (DFT) [7] using the Cambridge Serial Total Energy Package (CASTEP) code [8], the ultra-soft pseudopotential [9] is applied and the generalized gradient approximation (GGA) is used. The electron wave function is expanded in plane waves up to an energy cut-off of 380 eV, the Monkborst-Pack point mesh of 6×6×3 is employed for sampling the Brillouin zone after convergence test. The total energy stability is less than 1×10^{-5} eV/atom, the convergence accuracy of the interaction between atoms is 0.03eV/Å, the maximum interaction force is 0.05 GPa and the maximum displacement is 0.001 Å. The valence electrons involved in the calculation are $Ga\text{-}3d^{10}$, $Ga\text{-}4s^2$, $Ga\text{-}4p^1$, $N\text{-}2s^2$, $N\text{-}2p^3$, $In\text{-}4d^{10}$, $In\text{-}5s^2$, and $In\text{-}5p^1$, respectively.

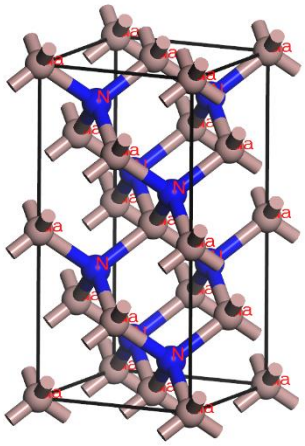

Figure 1. 1×1×2 supercell model of zinc blende GaN.

3. Results and discussion

3.1. The zinc blende GaN bulk structure

In order to compare the effect of In doping in zb-GaN, we firstly studied the electronic structure and photoelectric properties of the zb-GaN bulk structure. After optimization, the lattice constant is 4.558 Å, which is not much different from the experimental value [10] and other research results [11-12], the results and the calculation setting are proved to be reasonable. Then the electronic structure of the zb-GaN bulk structure is calculated, and the band structure, the total density of states (TDOS) and the partial density of states (PDOS) are discussed. The calculation results are shown in Figure 2 and Figure 3, respectively.

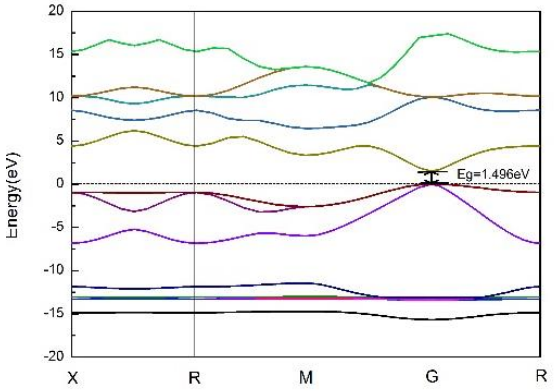

Figure 2. The band structure of zinc blende GaN.

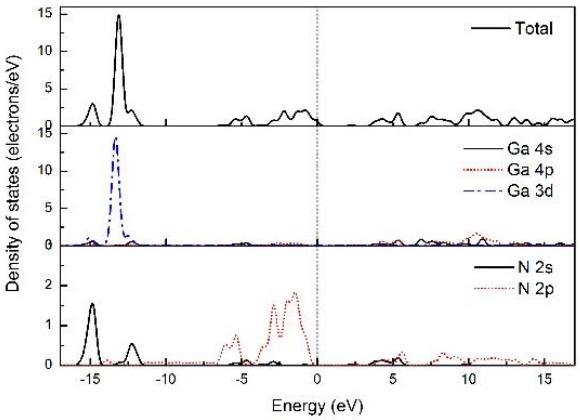

Figure 3. The total density of states and the partial density of states of zinc blende GaN.

It can be seen from Figure 2 that the conduction band bottom and the valence band top of zb-GaN are both at the *G* point of the Brillouin zone, indicating that zb-GaN is a direct band gap semiconductor. The band gap E_g=1.496eV, which is not much different from other research results [11-12], but smaller compared to the experimental value of 3.3eV [13]. This is because DFT does not consider the discontinuity of the exchange-correlation potential between electrons. Figure 3 illustrates that the DOS is mainly provided by *s*, *p*, and *d* orbitals and divided into three parts: -16~-11eV, -7~0eV, and 2~12eV, which is corresponded to the band structure in Figure 2, called the lower valence band, the upper valence band and the conduction band, respectively. The lower valence band is mainly contributed by the *Ga3d* state and the *N2s* state, in which the *Ga3d* state plays a decisive role. A sharp peak is shown at around -13.4eV, indicating that the locality of the region is relatively strong. The upper valence band is mainly contributed by *N2p* state, and the conduction band is mainly contributed by *Ga4s*, *Ga4p*, *N2s* and *N2p* state.

3.2. The In-doped zinc blende GaN structure

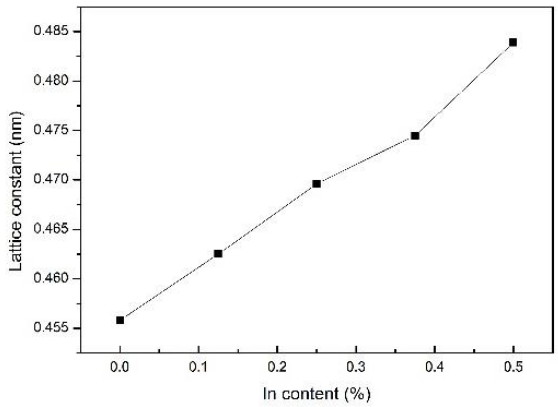

Figure 4. Lattice constant of $In_xGa_{1-x}N$ as a function of In content.

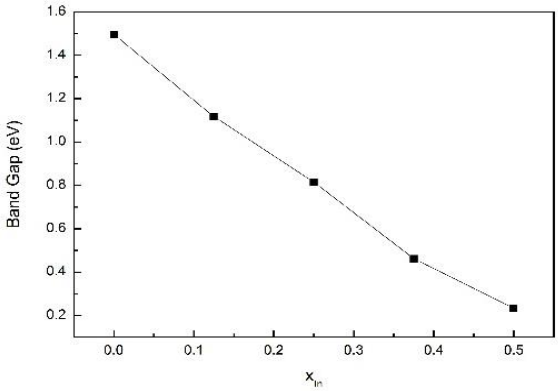

Figure 5. Band gap of $In_xGa_{1-x}N$ as a function of In content.

3.2.1. Lattice constant. The geometrically optimized zinc blende $In_xGa_{1-x}N$ has a lattice constant as a function of In content are shown in Figure 4. As the In content increases, the lattice constant *a* increases gradually. The reason is that the ionic radius of In (3.80 Å) is larger than that of Ga (3.62 Å), so the lattice expansion is caused when In atom is doped in situ at the position of Ga atoms.

3.2.2. Band gap and Density of states. Figure 5 shows the band gap of $In_xGa_{1-x}N$ as a function of In content. It is seen that the band gap E_g decreases with the increase of In content. In order to further explore the band gap variation of $In_xGa_{1-x}N$ system, the DOS and PDOS are discussed in Figure 6 below.

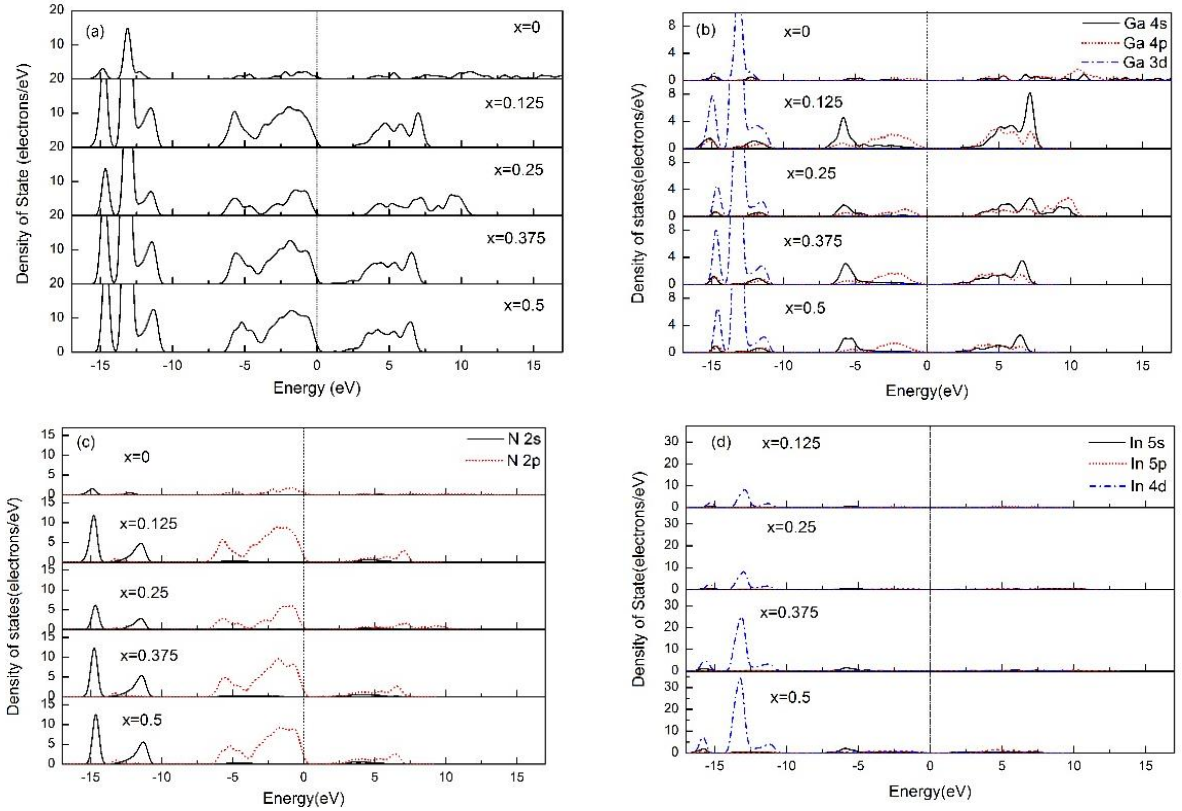

Figure 6. The density of states and the partial density of states of $In_xGa_{1-x}N$ at different x. (a) is the total density of states, (b) is the partial density of states of Ga atoms, (c) is the partial density of states of N atoms and (d) is the partial density of states of In atoms.

It can be seen from Figure 6(a)-(d) that the bottom of conduction band moves toward the low energy direction after In doping, and the peak intensity of the valence band and conduction band also increase as In content increases. For the lower valence band part, with the increase of In content, the effect of *Ga3d* state on the valence band is gradually reduced, while the effect of *In4d* state is increased. The two states interact with *N2s* state on the lower valence band, so that the locality of the region is obvious. For the upper valence band part, with the increase of In content, is still determined by *N2p* state and *Ga4s* state, in which *N2p* state plays a decisive role. The top of valence band is always determined by *N2p* state, and the position remains basically unchanged. As for the conduction band part, with the increase of In content, the peak density of the conduction band decreases, the conduction band and its bottom which *Ga4s* state dominated moves toward the low energy direction, so the band gap gradually decreases. It is worth noting that in the case of $x = 0.25$, the peak intensity of each band is lower than that of others (as shown in Figure 6 (a)). The range of the conduction band is affected by *Ga4s* state thus expanding towards to the high energy direction (as shown in Figure 6(b)).

3.2.3. Charge density difference. The reason that band gap decreasing can also be explained by the charge shifting shown in Figure 7. For un-doped GaN, the charge distribution around the atoms is uniform, exhibiting the properties of covalent bonds. For $In_{0.375}Ga_{0.125}N$, the charge between In and N is concentrated around In, showing the properties of strong ionic bonds. For Ga and N, the overlap of

electron cloud is reduced, resulting in a shift of *Ga4s* state to a low energy direction. With the doping concentration increases, the degree of shift increases and the band gap decreases.

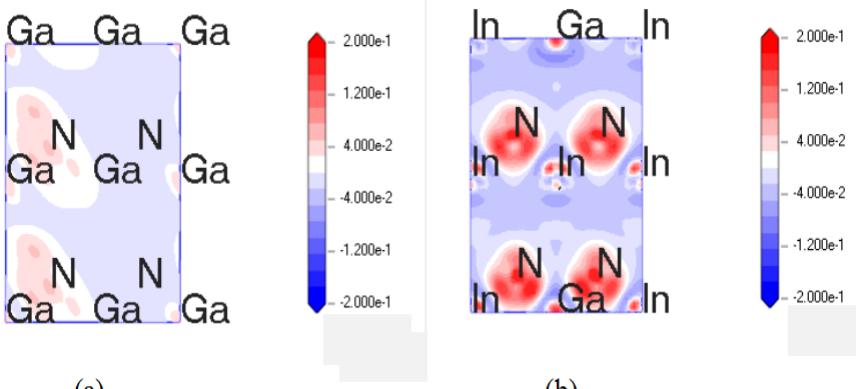

Figure 7. The charge density difference of (a)GaN and (b)$In_{0.375}Ga_{0.125}N$.

3.2.4. Optical properties. The absorption spectra of $In_xGa_{1-x}N$ at different x is shown in Figure 8 that the absorption coefficients increase firstly and then decrease as the wavelength increases. Pure GaN has an absorption wavelength range of 50nm-400nm, which is located in the far ultraviolet and ultraviolet regions, and the absorption peak intensity reaches the strongest about $4.7\times10^5 cm^{-1}$ near 104nm.

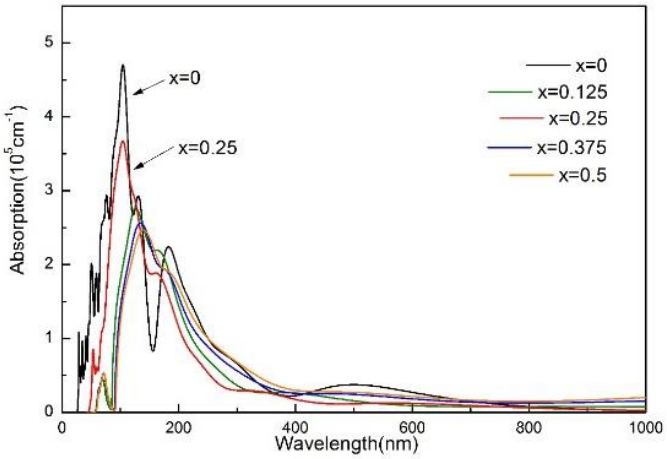

Figure 8. Absorption spectra of $In_xGa_{1-x}N$ at different doping concentrations x.

As the In content increases, (1) The absorption coefficient is reduced, and the strongest absorption peak moves toward the low energy direction. The reason is the increase of In content enhances the transition of electrons in *In4d* state towards to conduction band. (2) The absorption spectrum shows red shift. The absorption of visible light and part of infrared light by the $In_xGa_{1-x}N$ system is enhanced and the range becomes larger. Therefore, it can be inferred that by regulating the doping concentration, the absorption range of $In_xGa_{1-x}N$ can cover the entire solar spectrum. It is worth noting that the absorption peak of $In_{0.25}Ga_{0.75}N$ is larger than those of others (x=0.125, 0.375, 0.5), and the position of peak is red-shifted compared to pure GaN, while blue-shifted compared to other doping system. The reason is presumed to be the influence of *Ga4s* state, which brings about the expansion of the conduction band to high energy direction.

4. Conclusions

The electronic structure and photoelectric properties of zb-GaN with different In doping concentrations are calculated by first-principles. The results show that with the composition x increases, the lattice constant of InxGa1-xN increases and the band gap decreases, and the absorption spectrum shift to the red region. The light absorption range of InxGa1-xN alloys can cover the entire solar spectrum by adjusting the In content, therefore the InxGa1-xN can be used to fabricate photovoltaic devices such as full-spectrum solar cells.

Acknowledgement

This work was supported by the National Natural Science Foundation of China (61474030), the Guangxi Natural Science Foundation (2015GXNSFAA139265) and the Open Foundation of Key Laboratory of Nano devices and Applications, Chinese Academy of Sciences (15ZS06).

References

[1] Wu J, Walukiewicz W, Yu K M, et al. 2002 Unusual properties of the fundamental band gap of InN J. *Appl. Phys. Lett*. 80(21): 3967-3969
[2] Nakamura S. GaN growth using GaN buffer layer J. *Japanese Journal of Applied Physics*, 1991, 30(10A): L1705
[3] Chen Y, Wang W X, Li Y, et al. 2011 High Quality GaN Layers Grown on SiC Substrates with AlN Buffers by Metalorganic Chemical Vapor Deposition J. *Chinese Journal of Luminescence* 32(9):896-901
[4] Wang L, Ren F, Zhao W, et al. 2010 GaN grown on AlN/sapphire templates J. *Acta Physica Sinica* 59(11):8021-8025
[5] Okumura H, Ohta K, Feuillet G, et al. 1997 Growth and characterization of cubic GaN J. *Journal of Crystal Growth* 178(1–2):113-133
[6] Fabien C A M, et al. 2014 Guidelines and limitations for the design of high-efficiency InGaN single-junction solar cells *J. Solar Energy Materials & Solar Cells* 130:354-363
[7] Hohenberg P, Kohn W. 2017 Inhomogeneous Electron Gas *J. Resonance* 22(8):809-811
[8] Segall M D, Lindan P J D, Probert M J, et al. 2002 First-principles simulation: ideas, illustrations and the CASTEP code *J*. 14(11):2717
[9] Padilla J, et al. 1997 Ab initio study of $BaTiO_3$ surfaces *J. Phys. rev. B* 56(56):1625-1631
[10] Lei T, Moustakas T D, Graham R J, et al. 1992 Epitaxial growth and characterization of zinc-blende gallium nitride on (001) silicon *J. Journal of Applied Physics* 71(10):4933-4943
[11] Rao X, Wang R Z, Cao J X, et al. 2015 First-principles calculation of doped GaN/AlN superlattices *J. Acta Physica Sinica* 71(Pt2):262-270
[12] Qin H, Luan X, Feng C. Mechanical 2017 Thermodynamic and Electronic Properties of Wurtzite and Zinc-Blende GaN Crystals *J. Materials* 10(12):1419
[13] Guo J Y, et al. 2008 First-principles study on electronic structure and optical properties of Al and Mg doped GaN *J. Acta Physica Sinica* 57(6):3740-3746